

## A Simple Nozzle Analysis of Slow-Acceleration Solutions in 1-D Models of Rotating Line-Driven Stellar Winds

Stan Owocki

*Bartol Research Institute, University of Delaware, Newark, DE 19716*

**Abstract.** For a star rotating at more than about 75% of the critical rate, one-dimensional (1-D) models for the equatorial regions of a line-driven stellar wind show a sudden shift to a slow-acceleration solution, implying a slower, denser equatorial outflow that might be associated with the dense disks inferred for sgB[e] stars. To clarify the nature of this solution shift, I present here a simple analysis of the 1-D flow equations based on a nozzle analogy for the terms that constrain the local mass flux. At low rotation rates the nozzle minimum (or “throat”) occurs near the stellar surface, allowing a near-surface transition to a steeply accelerating, supercritical flow solution. But for rotations above about 75% of the critical rate, this *local*, inner nozzle minimum exceeds the *global* minimum approached asymptotically at large radii, implying that near-surface supercritical solutions would now have an overloaded mass loss rate. Maintaining a monotonically positive acceleration is then only possible if the flow is kept subcritical out to large radii, where the nozzle function approaches its *absolute* minimum. For fixed line-driving parameters, the associated enhancements in equatorial density are typically a factor 5-30 relative to the polar (or nonrotating) wind. However, when gravity darkening and 2-D flow effects are accounted for, it still seems unlikely that rotationally modified equatorial wind outflows could account for the very large densities inferred for the disks around supergiant B[e] stars.

### 1. Introduction

As hot, luminous supergiants, the sgB[e] stars are expected to have strong stellar winds, driven by line scattering of the star’s radiation, as modeled by the formalism introduced by Castor et al. (1975, hereafter CAK). A particular topic of discussion at this workshop centered on whether the dense equatorial disks inferred in such sgB[e] stars might just be associated with the enhanced wind outflow near the equatorial plane of a rapidly rotating star. In addition to the modest, factor-few enhancements in equatorial mass flux associated with a “bi-stability” shift in ionization at the lower temperature near the equator (Pelupessy et al. 2000), M. Curé has pointed out that at very high, near-critical rotation, the wind solution switches to a slow acceleration mode; the lower-speed outflow then implies a further enhancement in density, relative to the standard CAK, steep acceleration applicable at higher latitudes (Curé 2004; Curé & Rial 2004; Curé et al. 2005).

Spurred by these discussions, this paper aims to understand better the physical origin of these shallow wind acceleration solutions for high rotation rates. The basic approach applies a “nozzle analysis” originally developed to study disk-wind solutions (see, e.g., Pereyra et al. 2004). With a few judicious, but

quite reasonable approximations (e.g., neglecting gas pressure terms by taking the zero-sound-speed limit; using a beta velocity law to evaluate the finite-disk correction as an explicit function of space), it is possible to obtain simple integrations of the equation of motion to study the scalings of the mass loss rate with rotation, as well as the switch from steep to shallow acceleration solutions beyond a threshold rotation rate. Indeed, all the results and plots given here were computed with a few lines of simple *Mathematica* code<sup>1</sup>.

## 2. Scaled Equation of Motion

To begin, it is convenient to write the equatorial-plane equation of motion in a form that is scaled (see sec. 4 of Owocki 2004)<sup>2</sup> by the (electron-scattering-reduced) effective gravity  $GM_{eff}/r^2$ ,

$$(1 - w_s/w) w' = -1 + \omega^2(1 - x) + w_s/(1 - x) + fC_c \left( \frac{w'}{\dot{m}} \right)^\alpha. \quad (1)$$

The independent variable here is the inverse radius coordinate  $x \equiv 1 - R_*/r$ , while the dependent variable is the ratio of the radial kinetic energy to surface escape energy,  $w \equiv v^2/v_{esc}^2$ . Gas pressure effects are accounted for by terms containing the squared ratio of sound-speed (assumed constant in this isothermal model) to escape speed,  $w_s \equiv a^2/v_{esc}^2$ , which is typically very small, of order  $w_s \approx 10^{-3}$  in standard line-driven stellar winds. Centrifugal effects from rotation are characterized in terms of the ratio of the equatorial rotation speed to near-surface orbital (a.k.a. critical) speed,  $\omega \equiv v_{rot}/v_{orb} = \sqrt{2} v_{rot}/v_{esc}$ , under the assumption that wind material conserves its surface value of specific angular momentum,  $rv_\phi(r) = v_{rot}R_*$ . The scaled inertial acceleration is  $w' \equiv dw/dx = r^2v(dv/dr)/GM_{eff}$ .

Within the standard CAK formalism for line-driving, this acceleration also enters into the line-force, in proportion to  $w'^\alpha$ , where  $\alpha$  is the usual CAK power index. The overall normalization of this line force is cast here in terms related to the ‘‘point-star’’ CAK model, with  $\dot{m} \equiv \dot{M}/\dot{M}_{CAK}$  the ratio of the mass-loss rate to the point-star CAK value;  $C_c \equiv 1/(\alpha^\alpha(1 - \alpha)^{1-\alpha})$ ; and  $f$  the ‘‘finite-disk correction factor’’ (fdcf) given by eqn. (2) below. Note that for the non-rotating ( $\omega = 0$ ), zero-sound-speed ( $w_s = 0$ ), point-star ( $f = 1$ ) case of the classical CAK model, the critical solution (with maximal mass loss) is given by  $\dot{m} = 1$  and  $w(x) = x\alpha/(1 - \alpha)$ , implying a CAK mass loss rate  $\dot{M} = \dot{M}_{CAK}$  and a ‘‘beta-one-half’’ velocity law,  $v(r) = v_\infty(1 - R_*/r)^{1/2}$ , with terminal speed  $v_\infty = \sqrt{\alpha/(1 - \alpha)}v_{esc}$ .

## 3. Finite-Disk Correction Factor

Our goal is now to understand how the combined effects of the fdcf and rotation alter this classical CAK result. For a spherically symmetric wind, the radial

<sup>1</sup>The associated notebook is available via: [www.bartol.udel.edu/~owocki/xfr/rot-noz.nb](http://www.bartol.udel.edu/~owocki/xfr/rot-noz.nb)

<sup>2</sup>Available via: <http://www.bartol.udel.edu/~owocki/preprints/01eron-review.pdf>

variation of the fdcf is given by (see §VI of CAK),

$$f(r) = \frac{(1 + \sigma)^{1+\alpha} - (1 + \sigma\mu_*^2)^{1+\alpha}}{(1 + \alpha)\sigma(1 + \sigma)^\alpha(1 - \mu_*^2)}, \quad (2)$$

with  $\mu_* \equiv \sqrt{1 - R_*^2/r^2}$ , the cosine of the finite-cone angle of the stellar disk, and  $\sigma \equiv d \ln v / d \ln r - 1$ . For a rotating star and wind, this factor can be even more complicated, modified by the rotational shear of the wind outflow, and by the oblateness of the star and possibly also the equatorial gravity darkening of the source radiation (Gayley & Owocki 2000). However, for simplicity, we will base our analysis here on the spherical wind form given by eqn. (2). Indeed, even in this case, the complex dependence of this factor on the wind velocity and velocity gradient substantially complicates a full, self-consistent solution of the equation of motion (1) (Friend & Abbott 1986).

To make a further simplification that allows the fdcf to be evaluated as an *explicit* function of radius  $r$  (or inverse radius coordinate  $x$ ), let us thus assume the wind velocity law input into the fdcf can be well approximated by the simple “beta-law” form

$$v(r) = v_\infty(1 - R_*/r)^\beta. \quad (3)$$

Fig. 1 plots the resulting variation of  $f$  with the scaled coordinate  $x$  for various values of  $\beta$ . Note that the overall form is quite similar for all cases, increasing from a surface value  $f(R_*) = 1/(1 + \alpha)$  to past unity at the isotropic expansion radius (where  $dv/dr = v/r$ ),  $r/R_* = (1 + \beta)$  [corresponding to  $x = \beta/(1 + \beta)$ ], and eventually returning asymptotically to unity from above at large radii ( $x \rightarrow 1$ ). In the analysis below, we assume a fixed characteristic value of  $\beta = 1$  to evaluate the fdcf.

#### 4. Solving for Wind Acceleration in Terms of the “Nozzle Function”

Since gas pressure effects are typically small, of order  $w_s = 0.001$ , let us next consider the simplified limit of zero sound speed,  $w_s \rightarrow 0$ . A particularly convenient case is to take  $\alpha = 1/2$ , for which the equation of motion (1) becomes a simple quadratic equation in  $\sqrt{w'}$ ,

$$w' - 2f\sqrt{w'/\dot{m}} + g = 0, \quad (4)$$

where for convenience we have defined the reduced gravity as  $g \equiv 1 - \omega^2(1 - x)$ . We can then apply the quadratic formula to solve for a shallow (–) and steep (+) acceleration solution,

$$w'_\pm(x) = (g(x)n(x)/\dot{m}) \left[ 1 \pm \sqrt{1 - \dot{m}/n(x)} \right]^2, \quad (5)$$

where we have now finally defined the “nozzle function”,

$$n(x) \equiv \frac{f(x)^2}{g(x)} = \frac{f(x)^2}{1 - \omega^2(1 - x)}. \quad (6)$$

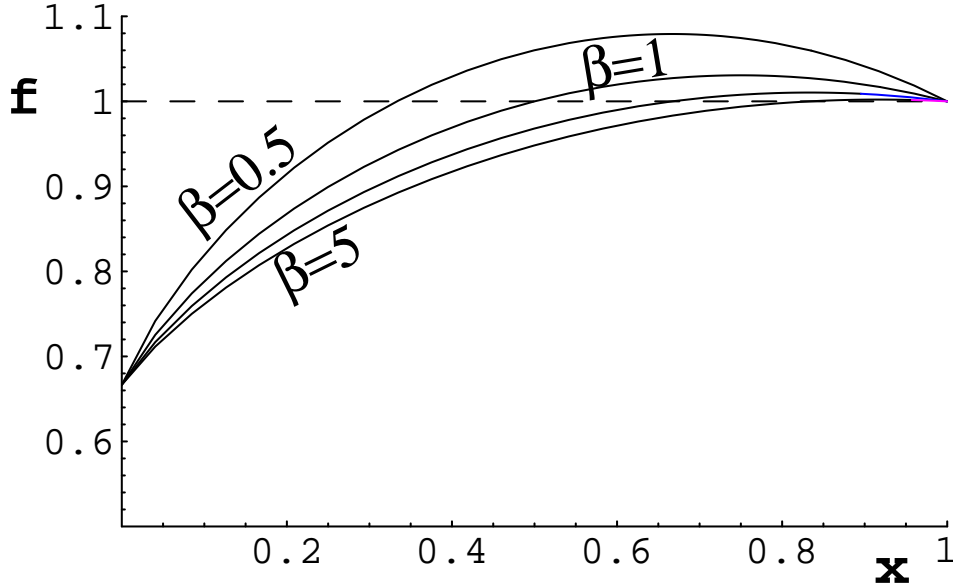


Figure 1. Spatial variation of the finite-disk-correction factor  $f$ , plotted vs. scaled inverse radius  $x = 1 - R_*/r$ , for CAK exponent  $\alpha = 1/2$  and various velocity-law exponents,  $\beta = 0.5, 1, 2,$  and  $5$ . The horizontal dashed curve denotes the unit correction that applies at the point of isotropic expansion (where  $\sigma = d \ln v / d \ln r - 1 = 0$ ), and at large distances where the star approaches the point-source form assumed in the original CAK model. A key point is that all these varied curves have a similar form, rising sharply from a base value [ $f_{d*} = 1/(1 + \alpha)$ ], crossing above unity (dashed line), and then relaxing back to it at large radial distances,  $x \rightarrow 1$ .

The significance of this nozzle function stems from its appearance with the mass loss rate  $\dot{m}$  within the square-root discriminant. In particular, we can readily see that maintaining a numerically real flow acceleration requires<sup>3</sup> a mass loss rate  $\dot{m} \leq \min[n(x)]$ . As such, the location of the global minimum of this function (the smallest nozzle “throat”) represents the *critical point* that sets the maximal allowed value of the mass loss rate,  $\dot{m} = \min[n(x)]$ , that is consistent with a monotonically accelerating outflow. Note that, at such a critical point, the discriminant in eqn. (5) vanishes, allowing the flow to transition smoothly from the sub-critical, shallow acceleration (–) root to a super-critical, steep acceleration (+) root.

Fig. 2 plots  $n(x)$  vs.  $x$  for various rotation rates  $\omega$ . Note that for no or low rotation (about  $\omega < 0.75$ ), the minimum of the nozzle function is less than unity, and occurs at the stellar surface,  $x = 0$ ; this allows the flow to transition

<sup>3</sup>Actually, this restriction really stems from our CAK scaling of the line-force with  $w'^\alpha$  (in this case  $\sqrt{w'}$ ), which requires a strictly *positive* acceleration,  $w' > 0$ . But if we provide a backup scaling for negative accelerations, e.g.  $g_{line} = 0$ , or  $g_{line} \sim |w'|^\alpha$ , then “overloaded” situations for which the square-root discriminant in eqn. (5) becomes negative simply lead to an abrupt switch, a so-called “kink” (Cranmer & Owocki 1996), to a negative acceleration, or “coasting” solution.

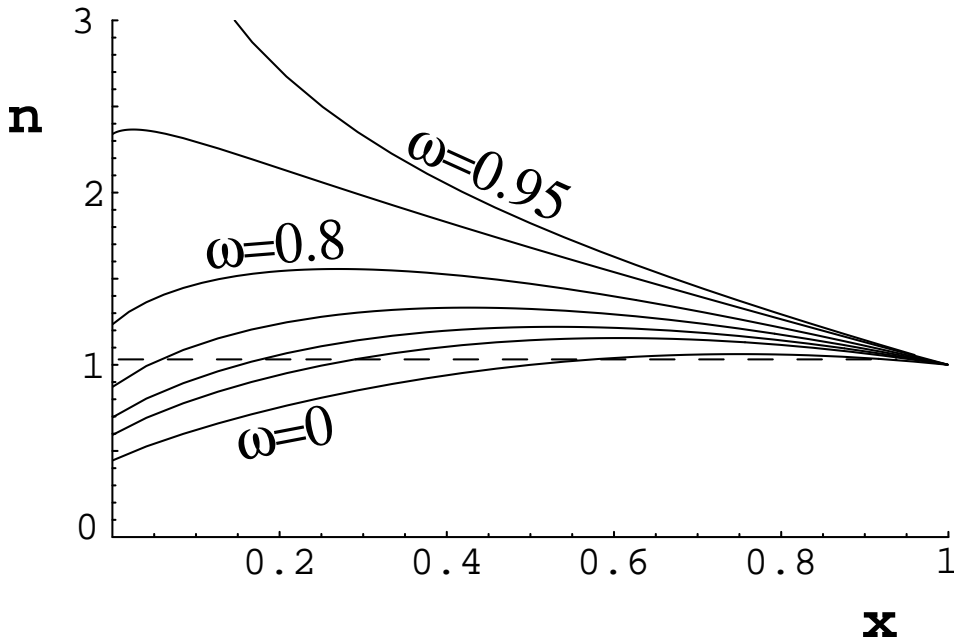


Figure 2. Nozzle function  $n(x)$  plotted vs. scaled inverse radius  $x = 1 - R_*/r$ , for various rotation rates  $\omega = 0, 0.5, 0.6, 0.7, 0.8, 0.9, 0.95$ , ranging from lowermost to uppermost. The horizontal dashed line at unit value represents the nozzle function for the CAK point-star model, with  $n = f = g = 1$ .

to a *super-critical* outflow directly from the static surface boundary condition  $w(0) = 0$ , following the steeper, plus (+) root for the acceleration in eqn. (5), but with a mass loss rate less than the point-star CAK value,  $\dot{m} < 1$ .

By contrast for large rotation rates (about  $\omega > 0.75$ ), the global minimum is unity, and occurs at large radii,  $x = 1$ ; satisfying the static surface boundary condition now implies that the flow at all finite radii should remain *sub-critical*, following the shallower, minus (–) root for the acceleration in eqn. (5), now with a mass loss rate just equal to the point-star CAK value,  $\dot{m} = 1$ .

## 5. Numerically Integrated Solutions for the Wind Velocity Laws

The associated wind velocity laws can thus be obtained by simple numerical integration of eqn. (5) from a static boundary  $w(0) = 0$ , following either the steep or shallow solution, depending on whether the rotation rate is high enough to shift the critical point (where  $n(x)$  has its absolute minimum) from the surface ( $x = 0$ ) to large radii ( $x = 1$ ). Fig. 3 plots the resulting velocity laws for selected slow vs. rapid rotation rates, yielding respectively the steep vs. shallow types of flow solution.

Fig. 4 illustrates the associated terminal speed and mass loss rates for these solutions, plotted as a function of rotation rate  $\omega$ , and again showing the abrupt shift from steep acceleration to shallow acceleration as the rotation increases

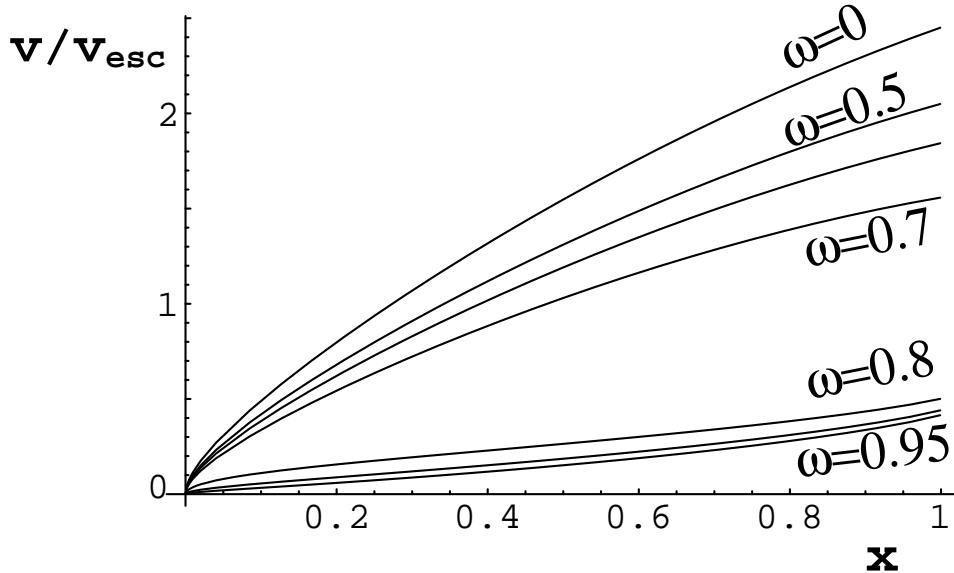


Figure 3. Flow speed over escape speed,  $v/v_{esc} = \sqrt{w}$ , plotted vs. scaled inverse radius  $x = 1 - R_*/r$ , showing a steep, supercritical acceleration for no or modest rotation,  $\omega = 0, 0.5, 0.6, 0.7$ , and shallow, subcritical acceleration for rapid, near-critical rotation,  $\omega = 0.8, 0.9, 0.95$ .

past the threshold rate at  $\omega \approx 0.75$ . Note that beyond this rotation, the mass loss saturates at the point-star CAK value,  $\dot{m} = 1$ .

These results also allow us to identify the radial variation of the relative density enhancement in the slow equatorial wind of a rotating star, compared to the non-rotating solution that applies to the polar wind. We are ignoring here gravity darkening and oblateness effects, as well as any bi-stability shift in the line-driving parameters between the polar and equatorial wind. From the above, the relative density enhancement is given by the ratio of the quantity  $\dot{m}/\sqrt{w}$  between the rotating and non-rotating models.

Fig. 5 plots the spatial variation of this density enhancement for rotating models with  $\omega = 0.8, 0.9$ , and  $0.95$ . Note that the enhancements are a few factors of ten, not insignificant, but not really sufficient to reproduce the inferred densities of B[e] disks, which are factors of order  $10^4$  or more denser than a typical polar wind outflow. Inclusion of bi-stability effects could give about another factor few by increasing the equatorial mass loss around the cooler, gravity-darkened equator. This thus might yield an overall enhancement of 100, which is again quite substantial, but still probably not sufficient to match the inferred values for B[e] star disks. Significantly higher enhancement would require an unrealistically low  $\alpha$  to further increase the equatorial mass flux, and/or assuming an equatorial surface rotation within a sound speed of the critical (orbital) speed. In the latter case, minor disturbances (e.g. pulsations) in the stellar envelope or photosphere could instead eject material into an orbiting, Keplerian decretion disk (Lee et al. 1991; Owocki 2005), obviating the need to invoke any central role for radiatively driven outflow solutions.

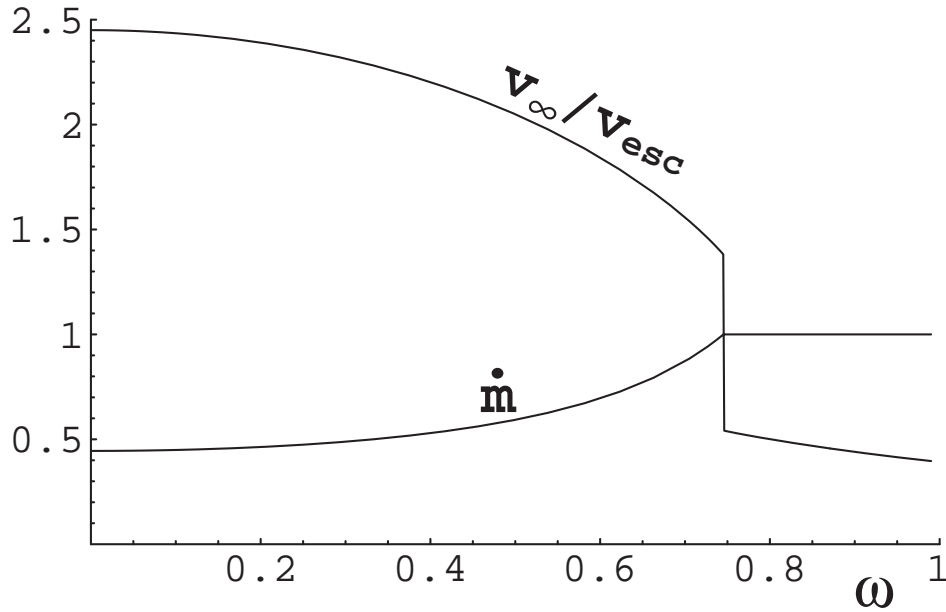


Figure 4. Upper curve: Terminal flow speed over escape speed,  $v_\infty/v_{esc} = \sqrt{w(1)}$ , plotted vs. rotation rate  $\omega$ , showing the shift from fast to slow wind as rotation rate is increased past ca.  $\omega = 0.75$ . Lower curve: Mass loss rate in units of point-star CAK value, again plotted vs. rotation rate  $\omega$ , showing the saturation at the CAK mass loss rate for rapid rotation,  $\omega > 0.75$ .

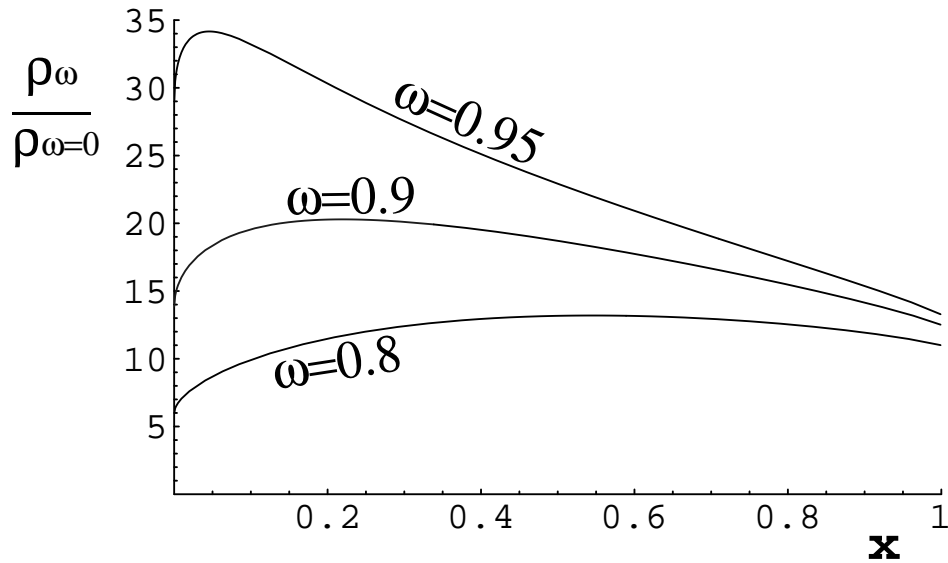


Figure 5. Density enhancement of slow wind solutions with rapid rotation rates,  $\omega = 0.8, 0.9,$  and  $0.95$ , relative to a non-rotating wind with the same wind parameters.

## 6. Discussion

The overall goal of this “nozzle analysis” is to clarify the physical reasons for the switch from a steep to shallow acceleration in 1-D line-driven wind models when the stellar rotation exceeds some threshold value, found here to be at  $\omega \approx 0.75$ . We see here that the central cause is the overloading of the base mass loss rate beyond the point-star, CAK value. Since the point-star, radial-streaming form of the line-force represents the optimal case for line-driving, the associated, point-star CAK mass loss rate represents the *maximal* mass loss (for a given set of opacity and stellar parameters) for which there can be a *monotonically accelerating* flow speed *throughout* the wind. The introduction of the fdcf reduces the effectiveness of the driving near the stellar surface, and thus reduces the maximal mass loss that can be initiated there. This reduction represents a kind of “safety” factor, allowing the outer wind to maintain a positive acceleration even as other effects, such as the centrifugal reduction in effective gravity near the surface, increase the base mass loss above its fdcf value. But as rotation increases beyond the threshold value  $\omega = 0.75$ , this base mass loss becomes greater than the point-star CAK value, and then the only globally accelerating solution possible is one with shallow acceleration, representing a slower, subcritical outflow.

This problem with wind overloading at large rotation rates was first noticed by Friend & Abbott (1986), who found indeed that beyond some threshold rotation rate, their super-critical, steep acceleration solutions could not be followed beyond some finite radius. The contributions of M. Curé and collaborators have since shown that this termination can be avoided by switching to a shallow acceleration solution. But it is not clear yet whether these shallow solutions will be local attractors in a time-dependent evolution, or whether perhaps they are inherently unstable. Indeed, the nonlinear nature of the equations can in principle accommodate a rich phenomenology regarding the attractor vs. unstable form of stationary solutions. Fortunately, there are already efforts underway to examine such cases with multiple minima in the nozzle function, originally motivated to understand the behavior of disk-wind solutions (A. Feldmeier, pc).

One should also add here a few words of caution about the physical relevance of such 1-D models. For example, the 2-D “Wind-Compressed-Disk” (WCD; see Bjorkman & Cassinelli 1993) simulations done in the mid-90’s (Owocki et al. 1994) show that, for moderately rapid rotation, there can be a 2-D flow pattern by which material from higher latitudes is focussed toward the equator through the WCD effect. Depending on whether the material reaches the equator above or below some “stagnation point”, it either drifts outward or falls back toward the star. Such simultaneous infall+outflow behavior is not possible in a steady 1-D model, but it is a perfectly natural outcome in a 2-D simulation. Of course, then there are also the issues of the non-radial line-force and how this affects the latitudinal motion of the flow, leading to inhibition of the WCD (Owocki, Cranmer, & Gayley 1996). Overall, it seems that a proper treatment of the role of rotation in inducing a denser, slower equatorial wind, must be examined from the context of at least 2-D models.

Finally, even beyond developing a 2-D CAK-type model, there remain key physical limitations not accounted for in this CAK formalism. Two examples are the intrinsic, small-scale instability of line-driving, and multiple scattering

effects. The former might well disrupt a slow-acceleration solution, even if the CAK form of such solutions should prove to be a stable attractor (J. Bjorkman, pc). The latter places strict upper limits on the mass flux that can be driven within a geometrically thin disk, since even with ideally tuned line-driving parameters within a CAK model (e.g. choosing an anomalously small CAK exponent  $\alpha$  to enhance the expected CAK-type mass loss rate), radiative driving in the thin disk would generally be limited to one or two scatterings before the photon escapes out of the disk plane. Thus, quite generally radiative driving could not produce a disk outflow that exceeds the single scattering limit. So, to the extent that observational inferences of sgB[e] disks imply a very dense medium (dense enough to form dust!), it seems more likely that these represent orbiting *Keplerian* disks, with perhaps ablation flows off the disk surface producing the equatorial outflow inferred by observations of Doppler-shifted absorption troughs in UV resonance lines.

**Acknowledgments.** This work was supported in part by NSF grants AST-0097983 and AST-0507581. I thank J. Bjorkman, M. Curié, A. Feldmeier, K. Gayley, T. Madura, and R. Nikutta for helpful discussions.

## References

- Bjorkman J. E., Cassinelli J. P., 1993, ApJ, 409, 429  
Castor, J. I., Abbott, D. C., & Klein, R. I. 1975, ApJ, 195, 157  
Cranmer, S. R., & Owocki, S. P. 1996, ApJ, 462, 469  
Curé, M., Rial, D. F., & Cidale, L. 2005, A&A, 437, 929  
Curé, M., & Rial, D. F. 2004, A&A, 428, 545  
Curé, M. 2004, ApJ, 614, 929  
Friend, D. B., & Abbott, D. C. 1986, ApJ, 311, 701  
Gayley, K. G., & Owocki, S. P. 2000, ApJ, 537, 461  
Lee, U., Osaki, Y., & Saio, H. 1991, MNRAS, 250, 432  
Owocki, S. P., Cranmer, S. R., & Blondin, J. M. 1994, Ap&SS, 221, 455  
Owocki, S. P., Cranmer, S. R., & Gayley, K. G. 1996, ApJ 472, L115.  
Owocki, S. 2004, EAS Publications Series, 13, 163  
Owocki, S. 2005, in *The Nature and Evolution of Disks Around Hot Stars*, R. Ignace & K. Gayley, eds., ASP Conf. Series, Vol. 337, 101.  
Pelupessy, I., Lamers, H. J. G. L. M., & Vink, J. S. 2000, A&A, 359, 695  
Pereyra, N. A., Owocki, S. P., Hillier, D. J., & Turnshek, D. A. 2004, ApJ, 608, 454